ARTICLE

Laser-induced Fluorescence Spectroscopy of NiO between 510 and 650 nm

Cheng-bing Qin, Jian-zheng Zang, De-ping Zhang, Qun Zhang*, Yang Chen*

Hefei National Laboratory for Physical Sciences at the Microscale and Department of Chemical Physics, University of Science and Technology of China, Hefei 230026, China

(Dated: Received on April 13, 2013; Accepted on May 7, 2013)

Laser-induced fluorescence excitation spectra of NiO have been recorded in the wavelength region of 510−650 nm under supersonic molecular beam conditions. More than fifty bands have been observed and rotationally analyzed to determine the molecular constants. The excited states exhibit highly irregular variations in terms of isotopic shifts, vibrational intervals, and rotational constants. Twenty-six bands attributed to [Ω=0, 1]-$X^3\Sigma_0^-$ transitions have been tentatively grouped into five vibrational progressions. Furthermore, dispersed fluorescence and lifetimes of the strong bands have also been measured.

Key words: NiO, Laser-induced fluorescence, Dispersed fluorescence

I. INTRODUCTION

Transition metal oxides have been extensively studied both experimentally [1−3] and theoretically [4−6] due to their interesting properties and important functionalities in many fields such as astrophysics [7], high-temperature chemistry [8], and materials science [9]. Most electronic spectra of 3d transition metal oxides have been well studied. Nevertheless, the spectroscopic data for NiO remain rather incomplete due to its numerous electronic states and extensive perturbations among these states. Just below 3.5 eV, Walch and Goddard have identified 26 electronic states arising from the first three atomic states of nickel and the ground-state oxygen [10]. Besides, the great changes in bond length between the excited and ground states were found to make the spectra of NiO possess weaker intensities than those of the earlier 3d oxides [11]. Therefore, so far only several excited states and the ground state of NiO have been well characterized.

The first spectrum of NiO was observed in 1945 by Rosen [12] using the exploding wire technique in the wavelength region of 400−950 nm, with all the observed bands grouped into six systems by vibrational analysis. Green and Reedy first determined the vibrational constants of the ground state by recording the infrared spectrum of matrix isolated NiO [13]. The first rotationally resolved spectrum in the green region was obtained by Srdanov and Harris who obtained precise ground-state constants [14]. Friedman-Hill and Field reported the $[16.0]^3\Sigma^-$-$X^3\Sigma^-$ and $[16.0]^3\Sigma^-$-$[4.3]^3\Pi_i$ bands by employing intra-cavity laser-induced fluorescence spectroscopy [15]. Ram and Bernath reported the $A^3\Pi_i^-$-$X^3\Sigma^-$ bands by means of Fourier transform infrared spectroscopy [16]. Molecular parameters of the ground and low-lying states were determined precisely. The pure rotational spectrum was observed and analyzed by Namiki and Saito using a source-modulated millimeter and submillimeter wave spectrometer [17]. The works mentioned above have identified the ground state to be a case $a^3\Sigma^-$ state. Recently, Balfour *et al.* have studied the NiO spectra between 410 and 510 nm via laser-induced and dispersed fluorescence spectroscopy [18]. More than 20 bands were rotationally analyzed for the first time.

In this work, we have extended the NiO spectra to a redder region, *i.e.* 510−650 nm, by means of laser-induced fluorescence (LIF) and dispersed fluorescence (DF) spectroscopy under supersonic molecular beam conditions. More than 50 bands were observed and analyzed, and reliable molecular constants were determined.

II. EXPERIMENTS

The production of a molecular beam sample of NiO was similar to that reported previously for other transition metal halide and sulfides [19, 20]. Briefly, the nickel atoms were sputtered, under a pulsed DC discharge condition, from a pair of sharp-head pin electrodes made of pure nickel metal. The NiO molecules were produced by reaction of the sputtered nickel atoms with O_2. The sample gas with ∼1%O_2 and 99%Ar at a stagnation pressure of approximately 6 atm passed through a pulsed nozzle (General Valve Co.) with an orifice diameter 0.5 mm into the vacuum chamber. The background pressure of the vacuum chamber was $\sim 3\times10^{-2}$ and $\sim 4\times10^{-4}$ Pa, with and without operation of the free jet, respectively. A relatively high stagnation pressure was used here to facilitate cold beam production.

*Authors to whom correspondence should be addressed. E-mail: qunzh@ustc.edu.cn, yangchen@ustc.edu.cn

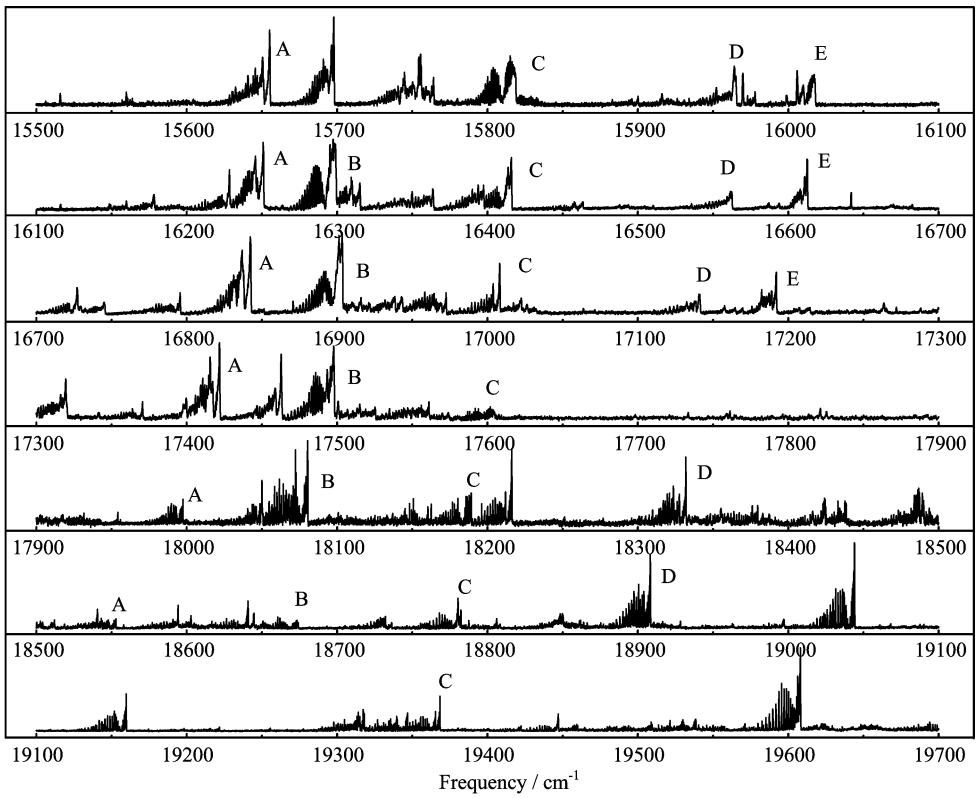

FIG. 1 The survey LIF exaction spectra of NiO in 15500−19700 cm^{-1}. Twenty-six observed vibronic bands grouped into five progressions are labeled by A, B, C, D, and E.

The nickel pins used for DC discharging the mixed O_2/Ar gas were fixed in a Teflon disk with an about 1.5-mm spacing and positioned at ∼2 mm downstream from the nozzle.

A tunable dye laser (Sirah, PRSC-LG-18) pumped by a Nd:YAG (Spectra Physics, GCR-190, repetition rate 10 Hz) was used to excite the jet-cooled NiO molecules. To cover the wavelength region of 510−650 nm, the C503, C540A, P597, and R640 (Exciton Inc.) dyes were used. The output of the pulsed dye laser (line width ∼0.2 cm^{-1}, pulse duration ∼8 ns) was introduced into the vacuum chamber and crossed the jet flow perpendicularly at ∼3.5 cm downstream from the point of DC discharge. The dye laser adopted a configuration of 1800 line/mm grating and a mirror. By using the second-order diffraction of the Littrow grating, better spectral resolution ∼0.1 cm^{-1} was obtained in 510−550 nm. Laser wavelengths were carefully calibrated by a wavemeter (Coherent, WaveMaster 33−2650, resolution ∼0.001 nm).

The fluorescence was collected by a pair of lens and detected with a photomultiplier tube (Hamamatsu, CR105) and then digitized by an A/D card interfaced to an acquisition computer. No attempt was made to normalize the LIF spectral intensity against the laser power. The relative time delays among the nozzle, the laser, and the discharge were controlled by a home-made pulsed multichannel delay generator. The DF spectra of NiO were obtained by fixing the probe laser frequency at a strong R-head and collected the fluorescence by a monochromator with the aid of a set of focusing lens. For lifetime measurements, a digital oscilloscope (Tektronix, TDS3032B) was used to record the fluorescence signal averaged over 128 laser shots.

III. RESULTS AND DISCUSSION

The survey LIF excitation spectra of NiO in the energy region of 15500−19700 cm^{-1} are presented in Fig.1. By using the second-order diffraction of the Littrow grating, better resolution has been obtained between 17900 and 19700 cm^{-1}, while the spectra in the region of 17600−17900 cm^{-1} show very low intensity because of the very low efficiency of the dyes. With a spacing of 600 cm^{-1}, the survey spectra were divided into seven parts, as shown in Fig.1, which will be discussed in detail later.

With the help of supersonic jet-cooled technique, the spectra turn out to be less congested and complicated than those reported in some previous studies [14, 15]. Even though the only lower level populated is the $X^3\Sigma_0^-(v{=}0)$, it gives rise to nearly 60 bands that can be rotationally resolved in this region. The NiO bands show two types of rotational structures: one with R, Q,

DOI:10.1063/1674-0068/26/05/512-518

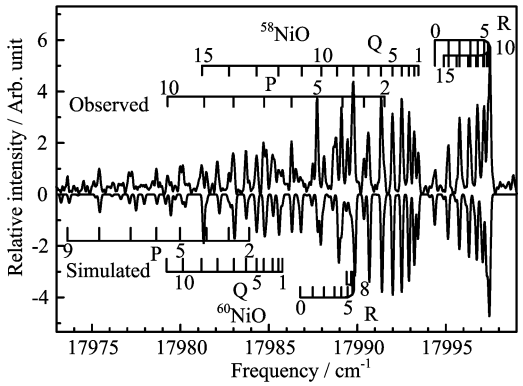

FIG. 2 Rotationally resolved LIF excitation spectrum of NiO attributed to the [Ω=1]-$X^3\Sigma_0^-$ transition. The upper (lower) trace is the observed (simulated) spectrum. Rotational assignments are indicated by ticks.

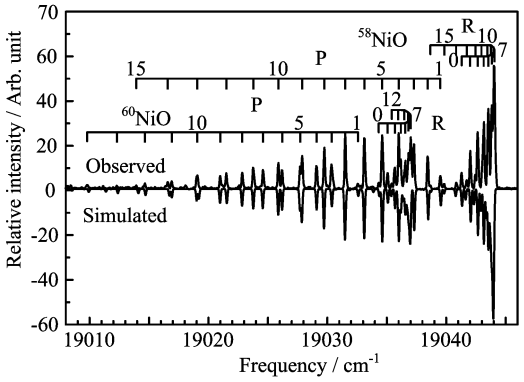

FIG. 3 Rotationally resolved LIF excitation spectrum of NiO attributed to the [Ω=0]-$X^3\Sigma_0^-$ transition. The upper (lower) trace is the observed (simulated) spectrum. Rotational assignments are indicated by ticks.

and P branches, and the other with R and P branches only. Rotational analysis indicated that they can be attributable to the [Ω=1]-$X^3\Sigma_0^-$ and [Ω=0]-$X^3\Sigma_0^-$ transitions, respectively. Typical rotationally resolved LIF excitation spectra with the two types of structures are presented in Fig.2 and Fig.3, respectively. In most instances an accompanying weaker band of similar structure can be seen slightly to the red shift of the strong band. Obviously, the appearance of such weak subband can be interpreted as a result of the isotopic shift between ^{58}NiO and ^{60}NiO, and the relative intensities of the two bands coincide with the natural abundant ratios of the two isotopologues, *i.e.* ^{58}NiO:^{60}NiO≈2.6:1.

The NiO molecular beam under investigation was well cooled down and vastly populated in the ground state due to a ∼100 μs expansion from the discharge zone to the detection zone. The DF spectra further confirm that all the LIF bands (except those with very weak features) can be ascribed to be from the $X^3\Sigma_0^-(v=0)$ as the lower level. Molecular parameters were obtained through a least-squares fitting procedure. The energies were modeled by the band origin (T_v), rotational (B_v), and centrifugal distortion (D_v) terms in the expression

$$F(J) = T_v + B_v[J(J+1)] - D_v[J(J+1)]^2 \qquad (1)$$

Even though the molecular constants of the ground state have been well determined from relatively high J'' values [14, 15, 17], the data from the jet-cooled source with the effective rotational temperature ∼40 K rarely gave measurable lines for J''>15, the fitting results show a relatively large root mean square (RMS) by using those constants for the lower state. The effective rotational constants for the ground state, B''=0.474882 cm^{-1}, was taken from the Balfour's work [18] and held fixed in our fitting. The D_v values taken from the microwave results [17] were fixed for both ground and excited states.

The least-squares fit was accomplished by the PGOPHER program [21]. The obtained parameters together with the isotopic shifts, *i.e.* $T_v(^{58}\text{NiO})$-$T_v(^{60}\text{NiO})$, are presented in Table I. Once the molecular parameters were determined, the simulated spectra can be given, as shown in the lower part of both Fig.2 and Fig.3, which match nicely with the observed spectra. Rotational assignments for the two isotopologues are also indicated, and the transition frequencies are listed in Table II.

Unfortunately, the excited states show highly irregular isotopic shifts and rotational constants provided by the rotational analysis, the vibronic assignments can not be given as those in other nickel containing molecules [19, 20]. The previous studies suggested that the vibrational intervals are ∼600 cm^{-1}, so the spectra were divided into seven parts with the spacing of 600 cm^{-1}, as shown in Fig.1. The spectral profile in these seven parts suggests five groupings of bands. A: A progression from 15651 cm^{-1}, namely the bands at 15651, 16246, 16838, 17417, 17993, and 18549 cm^{-1}. They all can be attributable to the [Ω=1]-$X^3\Sigma_0^-$ transition. The vibrational intervals are progressively 595, 592, 579, 576, and 556 cm^{-1}. B: A progression from 16291 cm^{-1}, namely the bands at 16291, 16897, 17492, 18076, and 18668 cm^{-1} with the [Ω=0]-$X^3\Sigma_0^-$ transition. Their corresponding isotopic shifts are 1.936, 2.560, 8.050, and 11.968 cm^{-1}, and the vibrational intervals are 606, 595, 584, and 592 cm^{-1}. Despite a similar spectral profile and a reasonable vibrational spacing, the 15694 cm^{-1} band was not assigned to progression B as it can only be assigned to the [Ω=1]-$X^3\Sigma_0^-$ transition. C: A progression from 15810 cm^{-1}, namely the bands at 15810, 16410, 17006, 17597, 18183, 18778, and 19364 cm^{-1} with the same Ω=0 for the upper states. These bands occur at intervals of ∼595 cm^{-1}, four of them have isotopic shifts of 2.125, 4.268, 8.177, and 3.00 cm^{-1}. The intensity of the 17597 cm^{-1} band was rather weak due to the low efficiency of the laser dyes. D: A progression from 15962 cm^{-1}, namely the bands at 15962, 16561, 17139, 18328, and 18904 cm^{-1} with the [Ω=0]-$X^3\Sigma_0^-$ transition. Their corresponding iso-

DOI:10.1063/1674-0068/26/05/512-518

TABLE I NiO band heads, band origins, rotational constants, isotopic shifts and lifetimes observed in LIF between 510 and 650 nm. The 1σ errors are given in parentheses in units of the last digits quoted.

No.	Head/nm	Ω'	T_v/cm^{-1}	B'/cm^{-1}	$\Delta\nu/\mathrm{cm}^{-1}$	$\tau/\mu\mathrm{s}$	Progression
1	638.77	1	15651.499(18)	0.42268(20)		2.558(11)	A: (v', 0)
2	637.03	1	15694.176(23)	0.42058(28)		2.524(8)	
		1	15692.710(20)	0.41723(20)	1.466		
3	632.17	0	15810.331(16)	0.45174(18)		1.873(8)	C: (v', 0)
4	626.40	0	15962.049(67)	0.40040(89)		1.214(4)	D: (v', 0)
5	624.31	1	16010.680(28)	0.44940(36)		1.225(6)	E: (v', 0)
6	616.21	1	16225.309(19)	0.41281(17)		3.110(20)	
7	615.36	1	16246.110(26)	0.43309(30)		2.541(8)	A: (v'+1, 0)
8	613.54	0	16291.863(21)	0.44664(25)		1.322(5)	B: (v', 0)
9	612.94	0	16310.020(13)	0.43334(21)		2.942(24)	
		0	16305.426(43)	0.43098(68)	4.594		
10	609.86	0	16393.686(45)	0.42047(49)			
11	609.18	0	16410.352(12)	0.43748(17)		1.752(4)	C: (v'+1, 0)
		0	16408.277(13)	0.43501(16)	2.125		
12	603.78	0	16560.641(75)	0.38145(69)		1.259(5)	D: (v'+1, 0)
		0	16558.199(84)	0.3809(13)			
13	602.63	1	16589.615(34)	0.42979(63)	2.442		
14	601.95	1	16608.455(31)	0.42898(39)		1.329(3)	E: (v'+1, 0)
		1	16605.517(54)	0.4252(11)	2.938		
15	598.47	0	16705.323(49)	0.42814(84)			
16	597.83	0	16723.750(31)	0.41956(55)		2.711(14)	
17	595.39	1	16792.481(17)	0.41623(13)		2.510(7)	
18	593.74	1	16838.296(20)	0.42645(18)		2.472(7)	A: (v'+2, 0)
		1	16833.263(55)	0.42391(72)	5.033		
19	591.60	0	16897.981(17)	0.43644(17)		1.164(3)	B: (v'+1, 0)
		0	16896.045(18)	0.43475(19)	1.936		
20	590.21	1	16938.708(30)	0.43074(38)		2.155(22)	
		1	16931.675(54)	0.42770(78)	7.033		
21	589.19	1	16968.848(13)	0.42058(14)		2.067(24)	
		1	16965.930(34)	0.41553(49)	2.918		
22	587.96	0	17005.579(17)	0.40178(25)		1.833(7)	C: (v'+2, 0)
		0	17001.311(43)	0.39893(65)	4.268		
23	583.39	0	17139.024(62)	0.38706(60)		1.385(20)	D: (v'+2, 0)
		0	17136.548(91)	0.38400(89)	2.476		
24	581.68	1	17187.322(17)	0.43265(19)		1.516(10)	E: (v'+2, 0)
		1	17183.997(24)	0.43039(25)	3.325		
25	579.26	0	17260.046(34)	0.42321(38)			
26	577.39	0	17314.346(12)	0.43541(21)		2.026(26)	
		0	17311.244(17)	0.43027(26)	3.102		
27	575.68	0	17367.301(21)	0.41814(19)			
28	574.74	0	17395.281(30)	0.42745(35)			
		0	17394.522(37)	0.41656(55)	0.759		
29	574.00	1	17417.580(27)	0.42782(26)			A: (v'+3, 0)
30	572.64	1	17459.042(28)	0.42528(37)		1.721(17)	
31	571.50	0	17492.542(21)	0.43642(24)		1.146(4)	B: (v'+2, 0)
		0	17489.982(34)	0.43488(57)	2.560		
32	568.03	0	17597.204(26)	0.44918(22)			C: (v'+3, 0)

DOI:10.1063/1674-0068/26/05/512-518

Table I continued.

No.	Head/nm	Ω'	T_v/cm^{-1}	B' / cm^{-1}	$\Delta\nu$/cm^{-1}	τ/μs	Progression
33	555.63	1	17993.630(16)	0.42404(13)			A: (v'+4,0)
		1	17985.956(21)	0.42085(25)	7.674		
34	554.01	1	18046.664(25)	0.42067(40)			
35	553.08	0	18076.807(16)	0.42302(10)		0.580(3)	B: (v'+3, 0)
		0	18068.757(23)	0.42341(32)	8.050		
36	549.78	0	18183.434(18)	0.44122(25)			C: (v'+4, 0)
		0	18175.257(24)	0.43572(28)	8.177		
37	548.96	0	18212.485(16)	0.42231(14)		0.618(4)	
		0	18208.596(31)	0.41643(41)	3.899		
38	545.74	0	18320.543(23)	0.41600(29)			
39	545.50	0	18328.333(21)	0.42256(21)		0.632(11)	D: (v'+4, 0)
		0	18324.028(25)	0.42056(33)	4.305		
40	539.35	0	18537.123(27)	0.41989(25)			
41	539.00	1	18548.907(11)	0.42695(13)			A: (v'+5, 0)
42	536.46	0	18637.272(14)	0.42000(20)			
43	535.50	0	18668.822(11)	0.43805(15)			B: (v'+4, 0)
		0	18656.854(42)	0.43676(47)	11.968		
44	532.47	0	18777.947(24)	0.40215(26)		0.432(2)	C: (v'+5, 0)
45	532.44	0	18778.915(63)	0.40267(66)			
46	528.87	0	18904.894(15)	0.41879(15)		0.771(3)	D: (v'+5, 0)
		0	18900.766(22)	0.41582(22)	4.128		
47	525.10	0	19040.614(18)	0.41855(14)		0.759(2)	
		0	19033.663(15)	0.41507(16)	6.951		
48	521.93	0	19156.439(17)	0.41813(14)		0.903(2)	
		0	19149.231(17)	0.41476(19)	7.208		
49	517.18	0	19331.834(25)	0.42314(33)			
50	517.07	0	19335.436(25)	0.42992(31)			
51	516.88	0	19342.926(47)	0.42400(60)			
52	516.30	0	19364.467(12)	0.42503(8)		0.443(4)	C: (v'+6, 0)
		0	19361.467(15)	0.42285(13)	3.000		
53		0	19444.388(11)	0.40596(11)		2.005(15)	
54 [18]	509.99	0	19604.989(20)	0.41349(16)		0.394(1)	
		0	19603.214(16)	0.40921(10)	1.775		
55 [18]	506.61	0	19736.247(20)	0.40502(20)		1.181(7)	
		0	19735.997(25)	0.40219(28)	0.250		

topic shifts are 2.442, 2.476, 4.305, and 4.128 cm^{-1}, and the vibrational intervals are 599, 578, 1189, and 576 cm^{-1}. It can be readily seen that the band between 17139 and 18328 cm^{-1} disappears due to the low efficiency of the laser dyes, as mentioned above. E: A progression from 16011 cm^{-1}, namely the bands at 16011, 16608, and 17187 cm^{-1} with the same Ω=1 for the upper states. Their corresponding isotopic shifts are 2.938, and 3.325 cm^{-1}, and the vibrational intervals are 597 and 579 cm^{-1}. Similarly to the recent works on NiO [18] and NiS [22], we group the 26 vibronic bands into the five progressions labeled A, B, C, D, and E in Fig.1 and Table I, respectively. In addition, the small isotopic shifts suggest small values of the vibrational quantum number in the excited states, *e.g.* $v'\leq$5, the exact values can not be determined by the irregular variations of their vibrational intervals, (see Fig.4) and the isotope shifts as well as the rotational constants.

It should be noted that the remaining 29 bands with considerable intensities in Fig.1 can neither be classified into any new groups easily nor the five progressions mentioned above. Nevertheless, since they can be well rotationally analyzed, the relevant molecular constants including band origins and rotational constants are also presented in Table I. In addition, as listed in Table I, some bands with appreciable spectral intensities can not be well rotationally analyzed due to severe spectral overlap and perturbations.

Furthermore, the DF spectra and lifetimes of the strong bands were measured. The lifetime was derived

DOI:10.1063/1674-0068/26/05/512-518

TABLE II Rotational assignments (in cm^{-1}) for the 555.63 nm band: $\nu-17900$ cm^{-1} and 525.10 nm band: $\nu-19000$ cm^{-1} of ^{58}NiO and ^{60}NiO. The 1σ errors are given in parentheses in units of the last digits quoted.

Band/nm	J	^{58}NiO			^{60}NiO		
		R(J)	Q(J)	P(J)	R(J)	Q(J)	P(J)
555.63	0	94.41(6)			86.61(−5)		
	1	95.16(5)	93.46(6)		87.49(8)	85.76(5)	
	2	95.77(1)	93.25(4)	91.53(2)	88.12(7)	85.54(2)	83.90(7)
	3	96.31(0)	92.96(1)	90.40(4)	88.66(6)	85.31(9)	82.74(5)
	4	96.78(3)	92.52(2)	89.10(0)	89.09(6)	84.87(4)	81.47(2)
	5	97.17(7)	91.98(2)	87.75(−1)	89.46(7)	84.31(−2)	80.14(3)
	6	97.38(4)	91.37(−4)	86.29(−2)	89.68(5)	83.71(−2)	78.64(−3)
	7	97.51(2)	90.62(−8)	84.69(−6)	89.78(1)	82.97(−6)	77.20(8)
	8	97.51(−2)	89.78(−12)	82.97(−13)	89.78(−3)	2.09(−14)	75.42(−7)
	9	97.43(7)	88.85(−14)	81.30(−5)	89.78(4)	81.19(−13)	73.62(−13)
	10	97.38(8)	88.10(12)	79.48(−1)	89.68(11)	80.36(4)	
	11	97.07(5)	86.80(−5)		89.33(3)	79.27(6)	
	12	96.68(12)	85.63(−1)		88.85(−7)	78.06(7)	
	13	96.13(13)	84.30(0)		88.44(1)		
	14	95.62(6)	82.74(−13)				
	15	94.90(15)	81.30(−2)				
	16	94.09(7)					
525.10	0	41.30(−5)			34.33(−5)		
	1	42.02(−5)		39.50(−6)	35.07(−2)		32.57(−4)
	2	42.65(−2)		38.45(−5)	35.69(2)		31.52(−3)
	3	43.15(−2)		37.28(−4)	36.18(−1)		30.36(−2)
	4	43.55(−1)		36.02(−1)	36.57(0)		29.09(−1)
	5	43.84(2)		34.62(−1)	36.84(1)		27.72(2)
	6	44.06(9)		33.12(1)	37.03(5)		26.20(0)
	7	44.06(6)		31.51(3)	37.03(7)		24.59(2)
	8	43.98(7)		29.76(3)	36.98(6)		22.85(1)
	9	43.77(7)		27.88(3)	36.79(8)		21.01(3)
	10	43.48(11)		25.89(2)	36.47(8)		19.05(5)
	11	42.97(6)		23.77(0)	35.97(2)		16.91(−1)
	12	42.46(13)		21.51(−2)	35.42(4)		14.66(−6)
	13	41.73(12)		19.05(−13)			12.29(−9)
	14	40.83(14)		16.58(−12)			9.80(−14)
	15	39.85(5)		13.93(−16)			
	16	38.68(0)					

from an exponential fit of the fluorescence decay traces. The lifetimes were found to range from 0.4 μs to 3.1 μs, as listed in Table I, which confirms extensive perturbations among the excited states investigated. The DF spectra were recorded with probe laser excitation coinciding with the most intense R-head. All the DF spectra recorded turned out to be quite similar. As an example, Fig.5 presented the DF spectrum with excitation laser wavelength at 509.99 nm (T_v=19604.989 cm^{-1}). The predominant emission was found exactly equivalent to the wavelength used for excitation, and no higher frequency was observed than the excitation laser, which implies that the excited state coming from the $X^3\Sigma_0^-(v''=0)$ level. The displacements of the five peaks in Fig.5, with respect to the position marked with a tick, read 0, 818, 2442, 3232, and 4009 cm^{-1}, respectively. The vibrational quantum numbers, v'', are also given. It is noteworthy that the v''=2 peak disappears. The similar irregular intensities were also observed by Balfour *et al.* who interpreted such an observation in terms of the Franck-Condon calculations using the established values for the ground state and the estimated parameters for the excited state, respectively [18]. The displacement frequencies were modeled by the following equation:

DOI:10.1063/1674-0068/26/05/512-518

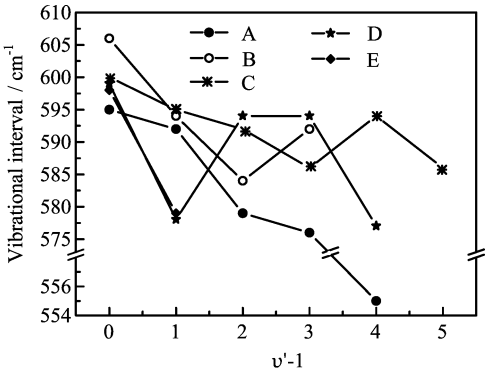

FIG. 4 Vibrational intervals for the five progressions *vs.* the vibrational quantum numbers of the excited state ($v'-1$). The third and forth intervals of progression D are the half of 1198 cm^{-1}.

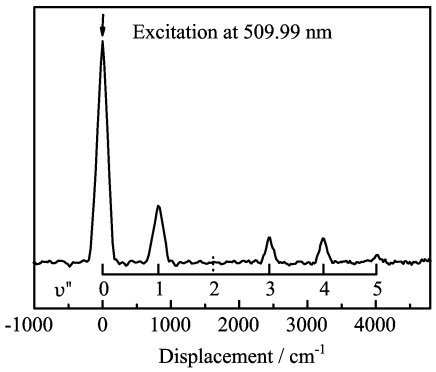

FIG. 5 The DF spectrum of ^{58}NiO obtained using a probe laser wavelength of 509.99 nm. The vibrational quantum numbers of the ground state, v'', are indicated by ticks.

$$G(v'') = \omega''_e \left(v'' + \frac{1}{2}\right) - \omega_e\chi''_e \left(v'' + \frac{1}{2}\right)^2 \qquad (2)$$

where ω''_e is the vibrational frequency, $\omega_e\chi''_e$ is the anharmonicity constant. Fitting the displacement values yields ω''_e=837±5 cm^{-1} and $\omega_e\chi''_e$=5.7±0.8 cm^{-1}, respectively. These two vibrational constants agree reasonably well with ω''_e=839.1(5) cm^{-1} and $\omega_e\chi''_e$= 5.4(5) cm^{-1} of Srdanov and Harris's work [14].

IV. CONCLUSION

The jet-cooled laser-induced fluorescence spectra of NiO have been investigated in the wavelength region of 510−650 nm, in which more than fifty bands were recorded and rotationally analyzed to determine the rotational constants and isotopic shifts. Highly irregular variations in terms of isotopic shifts, vibrational intervals, and rotational constants were observed, only twenty-six bands were grouped into five progressions by their vibrational intervals. Lifetime and dispersed fluorescence were also measured to gain more insights into the upper and lower states, and the vibrational constants of the ground state were determined.

V. ACKNOWLEDGMENTS

This work was supported by the National Natural Science Foundation of China (No.21273212 and No.21173205), the National Key Basic Research Program of China (No.2010CB923302), the Chinese Academy of Sciences (No.KJCX2-YW-N24), the Fundamental Research Funds for the Central Universities of China (No.WK2340000012), and the University of Science and Technology of China-National Synchrotron Radiation Laboratory Joint Funds (No.KY2340000021).

[1] Y. Endo, S. Saito, and E. Hirota, Astrophys. J. **278**, L131 (1984).
[2] D. A. Fletcher, C. T. Scurlock, K. Y. Jung, and T. C. Steimle, J. Chem. Phys. **99**, 4288 (1993).
[3] R. S. Ram, P. F. Bernath, S. P. Davis, and A. J. Merer, J. Mol. Spectrosc. **211**, 279 (2002).
[4] C. W. Bauschlicher, C. J. Nelin, and P. S. Bagus, J. Chem. Phys. **82**, 3265 (1985).
[5] A. J. Bridgeman and J. Rothery, J. Chem. Soc. Dalton Trans. 211 (2000).
[6] C. W. Bauschlicher and P. Maitre, Theor. Chim. Acta. **90**, 189 (1995).
[7] H. Spinrad and R. F. Wing, Annu. Rev. Astron. Astrophys. **7**, 249 (1969).
[8] A. J. Merer, Annu. Rev. Phys. Chem. **40**, 407 (1989).
[9] P. Poizot, S. Laruelle, S. Grugeon, and L. Dupont, J. M. Tarascon, Nature **407**, 496 (2000).
[10] S. P. Walch and W. A. Goddard, J. Am. Chem. Soc. **100**, 1338 (1978).
[11] M. Barnes, D. J. Clouthier, P. G. Hajigeorgiou, G. Huang, C. T. Kingston, A. J. Merer, G. F. Metha, J. R. D. Peers, and S. J. Rixon, J. Mol. Spectrosc. **186**, 374 (1997).
[12] B. Rosen, Nature **156**, 570 (1945).
[13] D. W. Green, G. T. Reedy, and J. G. Kay, J. Mol. Spectrosc. **78**, 257 (1979).
[14] V. I. Srdanov and D. O. Harris, J. Chem. Phys. **89**, 2748 (1988).
[15] E. J. Friedman-Hill and R. W. Field, J. Mol. Spectrosc. **155**, 259 (1992).
[16] R. S. Ram and P. F. Bernath, J. Mol. Spectrosc. **155**, 315 (1992).
[17] K. Namiki and S. Saito, Chem. Phys. Lett. **252**, 343 (1996).
[18] W. J. Balfour, J. Y. Cao, R. H. Jensen, and R. H. Li, Chem. Phys. Lett. **385**, 239 (2004).
[19] C. B. Qin, J. Z. Zang, Q. Zhang, and Y. Chen, Chin. J. Chem. Phys. **25**, 631 (2012).
[20] J. F. Zhen, L. Wang, C. B. Qin, Q. Zhang, and Y. Chen, Chin. J. Chem. Phys. **23**, 262 (2010).
[21] C. M. Western, *PGOPHER: A Program for Simulating Rotational Structure*, University of Birstol, http://pgopher.chm.bris.ac.uk.
[22] L. Wang, J. F. Zheng, J. Q. Gao, Q. Zhang, and Y. Chen, Chem. Phys. Lett. **493**, 245 (2010).

DOI:10.1063/1674-0068/26/05/512-518